Accurate control of a Bose-Einstein condensate by managing the atomic interaction

L. Morales-Molina[1,2] and E. Arévalo[2]

[1]*Departamento de Física, Facultad de Física, Pontificia Universidad Católica de Chile, Casilla 306, Santiago 22, Chile*

[2]*Max-Planck-Institut für Physik Komplexer Systeme, Nöthnitzer Str. 38, D-01187 Dresden, Germany*

(Received 15 February 2010; published 29 July 2010)

We exploit the variation of the atomic interaction in order to move ultracold atoms with attractive interaction across an ac-driven periodic lattice. By breaking relevant symmetries, a gathering of atoms is achieved. Accurate control of the gathered atoms' positions can be demonstrated via the control of the atomic localization process. The localization process is analyzed with the help of the *nonlinear Floquet states* where the Landau-Zener tunneling between states is observed and controlled. Transport effects in the presence of disorder are discussed.

DOI: 10.1103/PhysRevA.82.013642 PACS number(s): 03.75.Lm, 05.60.−k, 63.20.Pw

I. INTRODUCTION

In nonlinear discrete lattices, spatial discreteness and nonlinearity constitute the two main ingredients necessary for the existence of localized excitations. The existence and dynamics of these excitations can be understood from the analysis of their energy spectrum. In this spectrum, the localized states lie in gaps between bands of extended states.

The spectrum, and therefore the localized states, depend very much on the strength of the nonlinearity since the position and width of the bands and gaps vary with this parameter. In this respect, the nonlinearity strength can be used as a control parameter for tuning localized excitations. An ideal experimental testing ground for the application of this type of control is that of a Bose-Einstein condensate (BEC) trapped in a deep optical lattice, where much of the nonlinear and discrete effects can be probed in optical lattices [1].

Further control of matter waves (BEC) in optical lattices has been demonstrated with the use of fields; ac fields can modify the properties of the matter waves, by adjusting the parameters of the fields [2]. This is an intense and growing area of research, where examples of striking phenomena, such as transitions of a superfluid to a Mott insulator [3] and generation of directed transport [4,5], have found an experimental footing [6,7].

In this respect, a combination of ac fields together with management of nonlinearity opens new avenues for exploration of the new phenomena in BECs trapped in optical lattices.

In this work, we consider a general management of the atomic interaction for a BEC in the presence of an ac driving field. Manipulation of the atomic interaction is usually referred to as "management of Feshbach resonances" [8]. At these resonances, the scattering length undergoes large fluctuations with values going from positive to negative as the magnetic fields are tuned [9], thus opening many possibilities for the control of the atomic interaction. "Management" here refers to manipulation of dc and ac parts of the atomic interaction. The ac part is locally applied to induce motion of the atoms toward the perturbed sites. In light of new experiments, local variation of the atomic interaction is feasible by spatially modulating the interaction strength on a short-length scale [10]. Here, rather than focusing on the localization process itself, we analyze how to get transport of particles out of the localization process (i.e., how to transport cold atoms within optical lattices by controlling the location of the localization sites). Transport of matter waves has been reported to occur in the linear regime between defects [11]. We show below that the atomic interaction, whose strength can be easily tailored, also plays an important role in matter-wave transport by gathering atoms.

II. MODEL

Consider a lattice with periodic boundary conditions under the action of an ac force. The dynamics of a Bose-Einstein condensate with attractive interaction g can be described by the equation,

$$i\frac{d\varphi_n}{dt} - E_n\varphi_n + C(\varphi_{n+1} + \varphi_{n-1}) + g\,\varphi_n N_n - \varphi_n F_n(t) = 0. \tag{1}$$

where E_n is the energy at the site n. $N_n = N|\psi_n|^2$ is the population of atoms at the n^{th} site. N is the total number of atoms, that for convenience is normalized to 1. For the sake of dimensionless units, we set $\hbar = 1$. g accounts for the interaction strength between atoms, which is a function of the s-wave scattering length. This in turn can be tuned by means of magnetic fields [9]. More recently, control of the scattering length has been realized with a laser [10], allowing more accuracy and a less significant loss of atoms. $F_n(t)$ in Eq. (1) is a time-periodic real function reading as

$$F_n(t) = (-1)^n f(t) \equiv (-1)^n \eta \sin(\omega t), \tag{2}$$

with driving frequency ω and amplitude η. The term $(-1)^n$ accounts for the spatial periodicity of an optical lattice. The time-dependent function $F_n(t)$ mimics a flashing potential [6] for a discrete lattice. Equation (1) with (2) satisfies periodic boundary conditions only if the maximum number of lattice sites is even.

For $F_n(t) = E_n = 0$, Eq. (1) reduces to the well-known one-dimensional nonlinear Schrödinger equation,

$$i\frac{d\varphi_n}{dt} + C(\varphi_{n+1} + \varphi_{n-1}) + g\,\varphi_n N_n = 0. \tag{3}$$

Equation (3) has several stationary solutions, whose number depends on the number of sites in the lattice. Here, it is important to mention that, among these solutions, real symmetric and antisymmetric states can be observed [12]. In Eq. (1) the atomic interaction strength g can include dc and ac terms whose manipulation is usually referred to as "management of Feshbach resonances (MFR)" [8]. MFR has

proven to be an effective tool, on the mean-field level, for manipulation of cold atoms [8]. It has also been suggested as a way to control the tunneling process of a discrete number of atoms [13].

Notice, moreover, that the control of atomic population imbalances in a double-well potential has been realized by varying parameters in the system including the atomic interaction strength between atoms [14]. A similar kind of control has been proposed for controlling the wave packet spreading in a disordered lattice [15]. Upon varying the ramping speed of a linear time-dependent strength of the nonlinear term, the authors find optimum localization in the lattice in the presence of disorder.

From the perspective of a cold-atom system, localization, (namely gathering of atoms at few sites) implies a motion of atoms across the lattice, meaning a transport of particles. Notice that the process here is different from that of moving solitons, where the motion is achieved by kicking localized matter waves [16]. Motion of discrete solitons can also be assisted by nonlinearity management [17]. Thus, controlling the location of the localization sites allows us to control the transport of the atoms. With this aim, we consider dc and ac terms for g, namely,

$$g = g_0 + U\sin(\omega t + \theta), \tag{4}$$

where θ is a phase. It is expected that the periodic field in Eq. (2), along with management of the atomic interaction, may help to control localization of atoms at specific sites of the lattice.

In order to proceed it is convenient, for the sake of comparison with previously reported results [12], to take the complex conjugate of Eq. (1), namely,

$$i\frac{d\psi_n}{dt} + E_n\psi_n - C(\psi_{n+1} + \psi_{n-1}) - g\,\psi_n N_n + \psi_n F_n(t) = 0, \tag{5}$$

where $\psi_n = \varphi_n^\star$ ($\star$ stands for complex conjugation). Clearly, the complex conjugate of any solution ψ_n of Eq. (5) is a solution of Eq. (1). Moreover, by using the staggering transformation, $\psi_n = (-1)^n\psi_n'$ [18], in Eq. (5), we obtain an evolution equation for ψ_n' similar to Eq. (5) but with the sign in front of coupling constant changed (i.e., $C \to -C$). So, in this case, ψ_n' corresponds to solutions of a system where the repulsive interaction is present (see the following for further analysis).

A. Two-mode system

To gain an insight into the dynamics, it is convenient first to analyze the dimer lattice, which can be written as

$$i\frac{d\psi_1}{dt} = E\psi_1 + C\psi_2 + g\,\psi_1 N_1 + \psi_1 f(t), \tag{6}$$

$$i\frac{d\psi_2}{dt} = -E\psi_2 + C\psi_1 + g\,\psi_2 N_2 - \psi_2 f(t). \tag{7}$$

Here the energies are set as $E_1 = -E$ and $E_2 = E$, where E can be seen as a bias.

Equations (6) and (7) with $E = f(t) = 0$ have been used to describe the self-trapping transition of two weakly coupled BEC [19]. This phenomenon appears when the nonlinearity exceeds a critical value g_c [19,20].

To understand this phenomenon in the presence of an ac field $f(t)$, it is convenient to study the eigenfunctions of the extended Hilbert space of T-periodic functions, similar to that implemented in the linear regime (see Ref. [21]). Conventional Floquet theory fails in the presence of a nonlinear dependence on the wave functions. Nonetheless, Floquet states of the linear system can be traced into the nonlinear domain and new periodic orbits are found, which are then called nonlinear Floquet states [14,22–26]. The periodic solutions in the linear regime $g = 0$ fulfill the relation $|\psi_\beta(t)\rangle = e^{-i\varepsilon_\beta t}|\phi_\beta(t)\rangle$, where $|\phi_\beta(t+T)\rangle = |\phi_\beta(t)\rangle$ and ε_β is the quasienergy value.

In order to compute the nonlinear Floquet states, we use a numerical method implemented in the computation of breathers. First, we take a linear Floquet state as initial seed. The system is then perturbed with a small nonlinearity and the new state is found using a Newton-Ralphson iterative procedure by varying the initial seed. This is repeated by increasing the nonlinearity strength again by a small amount and updating the initial seed with the solution found in the previous convergence step. In each iteration step, the new trial function is integrated over a period of time. Conservation of the norm and variation of the quasienergy are imposed for the convergence to the desired solution. Technical details are given in Ref. [24].

The characterization of the localization process in the two-mode system, Eq. (6), can be done by observing the population imbalance between the two sites, which is defined as $S = |\psi_1|^2 - |\psi_2|^2$.

Equations (6) and (7) have two Floquet states for $g = 0$ with zero averaged population imbalances, namely $\langle S\rangle = 0$. We take then the Floquet state that for $f(t) = 0$ corresponds to the symmetric in-phase mode solution $\psi_1 = \psi_2 = (1/\sqrt{2})\exp(-iCt)$ [12,24] and trace it into the nonlinear domain. When increasing g above some g_c, the state bifurcates into three new states, as shown in Fig. 1(a). It is worth remarking here that for the staggering-transformation case, $\psi_n = (-1)^n\psi_n'$ [$C \to -C$ in Eqs. (6) and (7)], the Floquet state that bifurcates in the limit $f(t) = 0$ is the antisymmetric mode, [i.e., $\psi_1' = -\psi_2' = (1/\sqrt{2})\exp(-iCt)$]. This bifurcation point appears slightly shifted from $g_0 = 2$ (cf. with Fig. 1 in Ref. [12]) due to the presence in Eqs. (6) and (7) of a finite driving term $f(t)$ [i.e., $\eta \neq 0$ in Eq. (2)]. Two of these new states are degenerate, with opposite population imbalances. These are impossible to reach from the linear regime, because of the breaking of the adiabatic condition at the branching point [14]. For the analysis of the new states with nonzero population imbalances and its quantum mechanical counterpart in the limit $f(t) = 0$ we refer to Ref [27]. Let us now analyze the symmetries of Eqs. (6) and (7) in the presence of MFR [see Eq. (4)].

If $U = 0$ in Eq. (4), Eqs. (6) and (7) become invariant under the transformations:

$$S_1 : \psi_1 \to \psi_2, \quad t \to t + T/2, \tag{8}$$

and

$$S_2 : \psi_1 \to \psi_2, \quad t \to -t, \quad \text{complex conjugation}, \tag{9}$$

where S_1 corresponds to a generalized permutation symmetry.

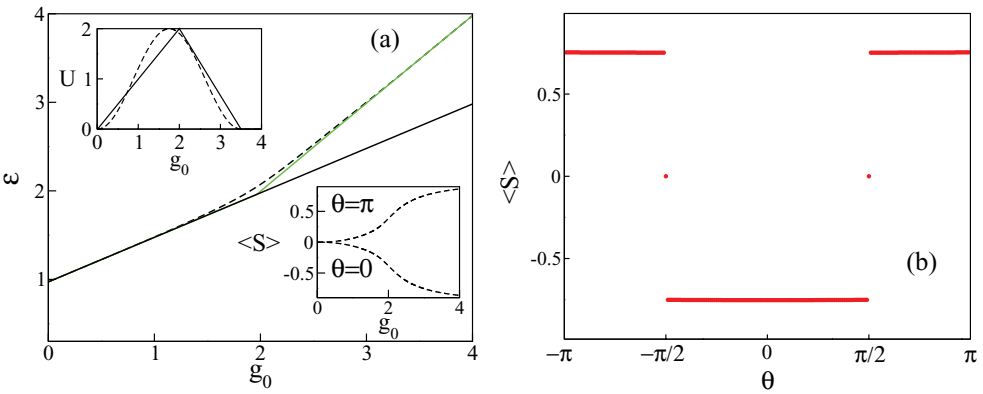

FIG. 1. (Color online) (a) Quasienergy ε versus g_0 for the two-mode system [Eqs. (6) and (7)]. Black and green (light gray) solid curves, $U = 0$; black dashed curve, $U^{\max} = 2$. (Top inset) Examples of pulse shape, U versus g_0: two-slope (solid line) shape and sine-square shape (dashed line). (Bottom inset) Average of population imbalance $\langle S \rangle$ versus g_0 for $U^{\max} = 2$. (b) $\langle S \rangle$ versus phase θ, $U^{\max} = 2$. The average $\langle \cdots \rangle$ is realized over a period $T = 2\pi/\omega$. Computations are performed with the sine-square shape depicted in the top inset of (a). The parameters are $C = 1$, $\omega = 2\pi$, $\eta = 1$, $E = 0$, $g_0 = 3$.

In contrast, for $U \neq 0$ the transformation S_1 is always broken while S_2 is broken only if $\theta \neq \pm\pi/2$.

Thus, taking Eq. (4) in Eqs. (6) and (7) with $\theta \neq \pi/2$, breaks both S_1 and S_2 symmetries.

The symmetries mentioned previously usually take place in ratchet systems. For instance, Eq. (9) is equivalent to a generalized time-shift symmetry (see, e.g., symmetries in Ref. [4,5]), whereas Eq. (9) is equivalent to a generalized time-reversal symmetry.

Breaking of symmetries by ac fields has shown to be useful in the generation of directed motion of atoms in optical lattices [6]. We shall show below that breaking of symmetries Eqs. (8) and (9), can help to control the atom's population in an optical lattice.

To follow states from the linear regime with zero population imbalances, it is convenient to modulate the ac nonlinear term U in Eq. (4) as a function of g_0, namely $U(g_0)$. In the following, we assume $U(g_0)$ has a pulse shape. As a result of this modulation, a new energy branch is created off the branching point that continuously join states with zero or little population imbalance to those states of strong population imbalances in Fig. 1(a). The pulse shape appears not to be very important, since the plots of the quasienergy curves obtained for pulses with two-slope and sine-square shapes [see top inset of Fig. 1(a)] show no significant difference. To reach those states with strong population imbalances, we simply ramp g_0 linearly in time, viz.

$$g_0(t) \equiv \alpha t, \tag{10}$$

where α is the speed of variation or ramping rate.

Here, care should be taken to not ramp g to values much larger than g_c, since fragmentation and lost of coherence can occur when the number of particles is low [28]. On the other hand, the number of particles should remain below a critical value to prevent the collapse of a condensate moving along a lattice [29]. Interestingly, changes of the phase θ creates states with opposite population imbalances, as shown in the bottom inset of Fig. 1(a). A full scan of the phase shows that the population imbalance becomes zero for $\theta = \pm\pi/2$ only [see Fig. 1(b)]. This is in agreement with the symmetry analysis from Eqs. (8) and (9). States with opposite population imbalances can therefore be selectively targeted when slowly changing g_0. Moreover, the smoothness of the new energy branch in the vicinity to the bifurcation point allows a significant increase in the ramping speed α. This is because a sharp variation in quasienergy is usually interpreted as a strong interaction with a very near eigenstate [30]. If the energy variation is smooth, high α values can be taken into account. However, for too high α, the system may hop from one state to other states with zero or little population imbalance. This implies a loss of localization. This jump brings to mind the Landau-Zener tunneling observed in the linear regime [30].

Furthermore, Eqs. (6) and (7) can describe the dynamics of opposite momenta for a condensate [24]. A generalization to an extended lattice, together with Landau-Zener tunneling between states of different momenta, may significantly change the transport of the atoms [24].

The previously mentioned technique comprises a rather general MFR [Eq. (4)] for the atomic interaction. Thus, we can partly summarize the main effects on the spectrum of quasienergies when the previously mentioned generalized management of the atomic interaction is applied: first, it creates a new quasienergy path that circumvents the branching point; second, the new path allows a rapid passage; and third, positive or negative strong population imbalance is reached upon choosing the phase θ.

So far, the analysis has been focused for a zero bias [i.e., $E = 0$ in Eqs. (6) and (7)]. For a nonzero bias $E \neq 0$, degeneracies are lifted as shown in the inset of Fig. 2. In this case, localization can also be achieved by slowly changing g_0 in time. In the same spirit as the functioning of a ratchet system [31,32], here we are interested in how localization is induced by means of ac fields and, more importantly, how this works against a bias. Our results show that the induced localization appears to work against a bias as shown in Fig. 2. An averaged nonzero population imbalance is induced for $E = 0$, whose effect survives for finite values of E. The offset is shifted to the right as the amplitude of the field $f(t)$, h, increases. Likewise, one can induce the same effect to the left by changing θ in $f(t)$ [Eqs. (6) and (7)].

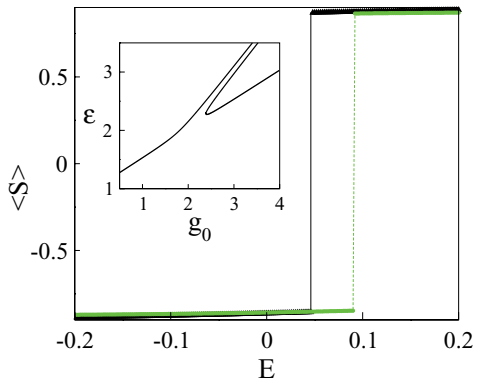

FIG. 2. (Color online) Average population imbalance $\langle S \rangle$ versus bias E for $U^{\max} = 2, \eta = 1$ (black), $\eta = 2$ [green (light gray)]; $g_0 = 4$, $\theta = 0$. We compute in the limit $\alpha = 0$. Computations are performed with the sine-square shape depicted in the top inset of Fig. 1(a). (Inset) Quasienergy ε versus g_0. The parameters are $C = 1, \eta = 1, E = 0.1$, and $U = 0$.

B. Lattice

As mentioned previously, states bifurcate in new branches, representing new solutions, as the nonlinearity strength increases. Hence, in order to describe the many possible solutions that appear in the system of Eqs. (1) and (2), as the nonlinearity increases, a shorthand description for each solution of the branch is convenient. Such analysis is usually realized in the limit of $g \to \infty$, where one can estimate the asymptotic solution $\boldsymbol{\psi} \equiv (\psi_1, \psi_2, \ldots)$, for every branch [12].

Rather than determine the solution $\boldsymbol{\psi} \equiv (\psi_1, \psi_2, \ldots)$, here we are interested in the average of the modulus squared of the wave function in the sites (i.e., $\langle |\psi_i|^2 \rangle$), that is, the average number of atoms localized at each site i. Thus, we take a modified shorthand representation, where now "•" accounts for the occupied sites with a $1/K$ fraction and "○" for a zero fraction of atoms of the corresponding state in the limit $g \to \infty$. Here, K is the number of nonzero ψ_i.

In the following, we consider a four-mode lattice. In this case, Eq. (1) for four sites remains invariant under permutations of the indices $1 \to 3$ and $2 \to 4$. Likewise, symmetries given by Eqs. (8) and (9) are also applicable. Figure 3 shows a section of the quasienergy spectrum versus nonlinearity strength. Of particular interest are the states {• • • •} with equal distribution of atoms across the lattice and {• ○ ○ ○}, with all the atoms localized in one site.

We consider now the MFR [Eq. (4)] which creates as mentioned above, a new branch that joins the zero-population state with that of very high-population imbalance as g_0 increases (Fig. 3, dashed line).

Interestingly, as the pulse of the ac nonlinearity strength $U(g_0)$ is applied on two sites only, the number of atoms tends to localize in one of these two sites when ramping g_0, meaning that a motion of atoms from all the other sites to this new populated site has taken place. This can be fully controlled with the phase θ [see Eq. (4)]. In this respect, the combined action of ramping g_0 along with an ac perturbation of g [see Eq. (4)] can, in principle, help to control the movement of atoms along the lattice. Figure 4 schematically shows a method to move atoms from one lattice site to another. The

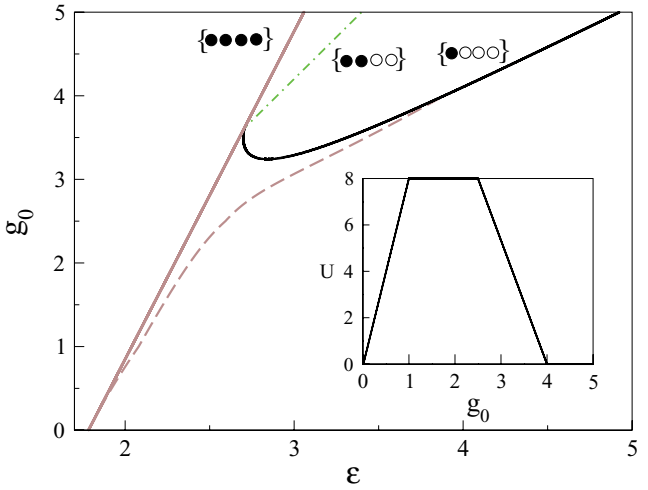

FIG. 3. (Color online) Nonlinearity strength g_0 versus quasienergy ε for $n = 4$. $\eta = 4$. Dashed line is a quasienergy state that results from continuing the linear Floquet state into the nonlinear domain, in the presence of an ac pulse of the nonlinearity strength, with the profile shown in the inset. (Inset) Pulse profile U versus g_0, $\omega = 4\pi$, $C = 1$.

lower graphic depicts two stages in time, each one consisting of two ramping process of g_0, which are described as follows: As time proceeds g_0 increases until it reaches a maximum value $g_0^{\max}$ at $\tau = g_0^{\max}/\alpha$, where a localization of atoms takes place. Afterward, g_0 is ramped down in time until $g_0 = 0$ at 2τ (at this point the number of atoms is equally distributed). At the second stage, the ac perturbation is applied on two sites, different from the prior ones, thus making atoms gather in a different new lattice location. In doing so, we have effectively achieved moving atoms from one lattice site to another at time 3τ. The entire process of moving atoms to different sites in a circular ring is depicted in the top part of Fig. 4 by a sequence of drawings. Each drawing represents a configuration of localization of atoms in the ring at the end of every ramping process. The black color on one site stands for a large concentration of atoms at this site, whereas absence of color represents a zero or very low number of atoms. Drawings with brown (lighter) color at every site means an equal distribution of atoms. Notice that this process can be repeated over and over, to shift atoms to any target site of the lattice.

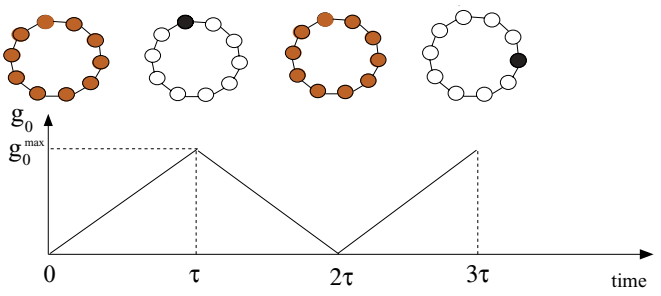

FIG. 4. (Color online) (Bottom) Sketch of the ramping process. (Top) Distribution of atoms in a ring of connected sites at the beginning and end of every ramping process. (For meaning of colors see text).

A remaining open issue is why the atoms initially distributed in the whole lattice gather at a single site. Though it is clear that motion takes place via a tunneling process of atoms across the lattice, the way the atoms tunnel may involve not only single-order tunneling (tunneling of a single particle) but also higher orders of tunneling (tunneling of bound particles) [33].

Up to now, the analysis has been focused on the manipulation of atoms at the level of Floquet states. Clearly, to steer atoms in the lattice, one needs first to populate those states. Population of the Floquet state where atoms appear equally distributed across the lattice is realized by "slowly" turning on the periodic field, using a uniform distribution of atoms as the initial condition. For a uniform distribution, we take the wave function $\psi = \frac{1}{\sqrt{J}}(1,1,1,\ldots)$, where J is the number of lattice sites. We ramp then the $f(t)$ amplitude, η [Eq. (2)], from 0 to its maximum value. This process is carried out at a speed α_f that satisfies the constraint $\alpha_f/\omega \ll 1$. In the staggering-transformation case, $\psi_n = (-1)^n \psi'_n$ [$C \to -C$ in Eq. (5)], the localization process is achieved by taking the staggered wave function $\psi' = \frac{1}{\sqrt{J}}(1,-1,1,\ldots)$, as the initial condition.

In what follows, we consider a lattice of 20 sites. In Fig. 5 the atom number distribution is recorded after ramping up g_0 during the two consecutive stages, as depicted in Fig. 4. Notice the apparent localization of atoms on the sites that are perturbed by the ac pulse $U(g_0)$ [see Eq. (4)]. In the first stage, the ac pulse is applied on sites 2 and 3 and localization takes place on site 3. In the second stage, the ac pulse acting on sites 13 and 14 causes localization on site 13. The localization on the perturbed sites depends on θ similarly as in Fig. 1 for the two-mode system.

A question that arises is whether this procedure can be applied to much larger lattices, and which limitations exist. From the quasienergy analysis, more sites in the lattice implies more Floquet states in the quasienergy spectrum with energies becoming more densely packed and with smaller energy gaps. This increases the probability for Landau-Zener transitions, thus decreasing the control over the atoms. Indeed, further numerical tests indicate that the movement of atoms is possible for a lattice with a larger number of sites, at the expense of reducing the ramping speed. The larger the lattice becomes, the longer the time is needed for the atoms to move across the lattice and gather together at few sites.

In the scenario of 20 sites, shown in Fig. 5, localization at specific sites is achieved by ramping speeds α as large as $\alpha_c = 1.95 \times 10^{-2}$. However, the transfer of atoms in the lattice from one site to another different one requires a lower speed with a value lower than or equal to $\alpha_a = 9 \times 10^{-3}$. For this α_a value, for example, the dimensionless time "t" needed for the process of localization (region $0 \leqslant t \leqslant \tau$ in Fig. 4) and transfer of atoms from one site to another one (region $\tau \leqslant t \leqslant 3\tau$ in Fig. 4) is approximately 1650 if $g_0^{\max} = 5$. By rescaling back this dimensionless value to seconds (s), with the help of the relation $\bar{t} = t/8\omega_r$ [34] and recoil frequency $\omega_r = 2\pi \times 25\,\mathrm{kHz}$, we obtain the value $\bar{t} = 1.32 \times 10^{-3}$s. This is an experimentally feasible value, which could be observed in experiments of ultracold atoms.

We have shown for a two-mode system that localization may take place against a bias. Lattice impurities cause a similar effect in the energy spectrum to that of a bias for a dimer setting (cf. bifurcation in Ref. [35] with inset in Fig. 2). So, it is of particular interest to see what happens with the movement of atoms from one site to any other site in the presence of impurities.

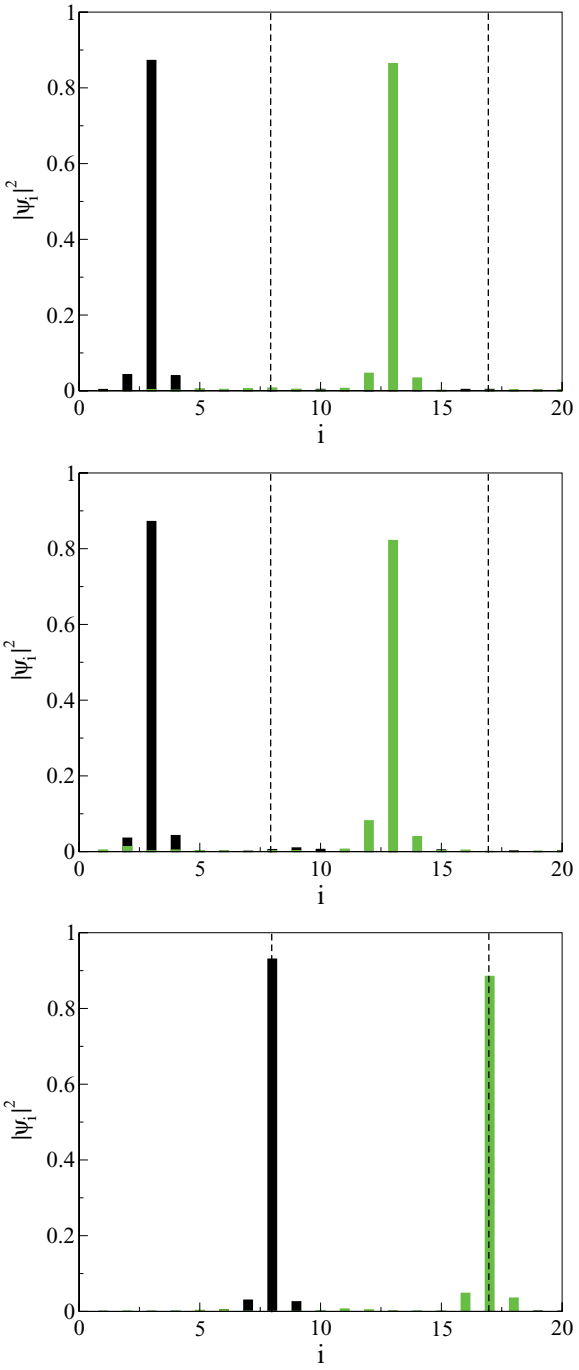

FIG. 5. (Color online) Atoms density $|\psi_i|^2$ versus location site i. Black and green (light gray) indicate first and second localization, respectively. (Top) $Q = 0$; (middle) $Q = 0.025$; (bottom) $Q = 0.05$. The dashed lines indicate the impurities location at the sites $i = 8,17$. (See text for details on the localization sites.) $C = 1$, $\omega = 4\pi$, $\eta = 4$, $\alpha_f = 0.1$, $\theta = \pi$, $\alpha = 5 \times 10^{-3}$, $g_0^{\max} = 5$. Computations are performed with the $U(g_0)$ shape depicted in the top inset of Fig. 3.

Here, we consider two impurities placed between the initial and final sites of the motion process. The impurities are introduced by changing the energies at some specific sites [i.e, $E_n = -Q(\delta_{n,k} + \delta_{n,m})$], where $\delta_{n,i}$ is the Kronecker's delta function. k and m are the indices of the impurity sites in a lattice that runs from $n = 0, \ldots, 20$ and Q is the absolute amount of energy at those sites. For low Q, movement of atoms takes place as in the homogeneous lattice, whereas for large Q, the atoms tend to localize at the impurity sites, shown in Fig. 5.

We performed similar computations with a random distribution of impurities (not shown). The results observed are similar to those exhibited above, where the atoms tend to gather at impurities with large E_n.

C. CONCLUSIONS

In summary, we have shown the steering of a Bose-Einstein condensate with a generalized management of the atomic interaction in a nonlinear discrete ac-driven lattice. Transport of atoms is realized via the control of the atom's localization process. The whole process relies on gathering atoms in different sites of the lattice upon successive ramping move-in time of a dc part of the atomic interaction strength.

Localization of atoms is achieved upon ramping the atomic interaction assisted by an ac field, together with periodic oscillations of the nonlinear interaction. This process of localization is first explained within a two-mode approximation, where the sign of the population imbalances is controlled by the phase of the periodic functions. This is supported by a symmetry analysis. We also show within a two-mode setting that control of the localization, created by the application of ac perturbations, may overcome a bias.

This was later shown to be feasible in the lattice, when movement of atoms was proven to be robust against a low intensity of disorder.

The control procedure exposed here paves the way for further application in other nonlinear systems, such as nonlinear optics where the nonlinearity strength is modulated [36] (see also references therein). Likewise, these results can be used for a generic equation like the discrete self-trapping equation with application to fundamental problems, such as dynamics of small molecules [37], dynamics of molecular crystals [38], among others. On the other hand, similar management of the atomic motion may be potentially useful in the control of momenta states in a condensate and consequently for the transport of ultracold atoms in optical lattices.

Our results were obtained via a discrete nonlinear Schrödinger equation which is bound to the validity of the mean-field approach. In this regard, experiments on BEC have provided enough evidence of the validity of the mean-field approach, as, for example, the asymmetric Landau-Zener tunneling in a periodic potential [39]. Therefore, it would be of great interest to conduct experiments with the aim of probing the role of the Landau-Zener tunneling in the localization process of atoms in a periodic lattice as the nonlinearity strength is ramped.

ACKNOWLEDGMENTS

The authors are grateful to fruitful comments on symmetries by Sergej Flach and also to suggestions by Joshua D. Bodyfelt. L.M.-M. is grateful for the hospitality of the Max-Planck-Institut für Physik Komplexer Systeme. L.M.-M. acknowledges financial support from Mejoramiento de la Calidad de la Educación Superior (Mecesup) of Chile.

[1] O. Morsch and M. Oberthaler, Rev. Mod. Phys. **78**, 179 (2006).
[2] A. Eckardt and M. Holthaus, Journal of Physics: Conference Series **99**, 012007 (2008).
[3] A. Eckardt, Ch. Weiss, and M. Holthaus, Phys. Rev. Lett. **95**, 260404 (2005).
[4] S. Denisov, L. Morales-Molina, and S. Flach, Europhys. Lett. **79**, 10007 (2009).
[5] S. Denisov, L. Morales-Molina, S. Flach, and P. Hänggi, Phys. Rev. A **75**, 063424 (2007).
[6] T. Salger *et al.*, Science **326**, 1241 (2009).
[7] H. Lignier, C. Sias, D. Ciampini, Y. Singh, A. Zenesini, O. Morsch, and E. Arimondo, Phys. Rev. Lett. **99**, 220403 (2007).
[8] P. G. Kevrekidis, G. Theocharis, D. J. Frantzeskakis, and B. A. Malomed, Phys. Rev. Lett. **90**, 230401 (2003); F. K. Abdullaev, E. N. Tsoy, B. A. Malomed, and R. A. Kraenkel, Phys. Rev. A **68**, 053606 (2003); H. Saito and M. Ueda, Phys. Rev. Lett. **90**, 040403 (2003).
[9] S. Inouye *et al.*, Nature **392**, 151 (1998).
[10] D. M. Bauer, M. Lettner, Ch. Vo, G. Rempe, and S. Dürr, Nature Physics **5**, 339 (2009).
[11] Ch. Weiss, Phys. Rev. B **73**, 054301 (2006).
[12] J. C. Eilbeck, P. S. Lomdahl, and A. C. Scott, Physica D **16**, 318 (1985).
[13] J. Gong, L. Morales-Molina, and P. Hänggi, Phys. Rev. Lett. **103**, 133002 (2009).
[14] L. Morales-Molina and J. Gong, Phys. Rev. A **78**, 041403(R) (2008).
[15] R. A. Vicencio and S. Flach, Phys. Rev. E **79**, 016217 (2009).
[16] E. Arévalo, Phys. Lett. A **373**, 3541 (2009).
[17] J. Cuevas, B. A. Malomed, and P. G. Kevrekidis, Phys. Rev. E **71**, 066614 (2005).
[18] M. Johansson and Y. S. Kivshar, Phys. Rev. Lett. **82**, 85 (1999).
[19] A. Smerzi, S. Fantoni, S. Giovanazzi, and S. R. Shenoy, Phys. Rev. Lett. **79**, 4950 (1997).
[20] S. Aubry, S. Flach, K. Kladko, and E. Olbrich, Phys. Rev. Lett. **76**, 1607 (1996).
[21] H. Sambe, Phys. Rev. A **7**, 2203 (1973).
[22] M. Holthaus, Phys. Rev. A **64**, 011601(R) (2001).
[23] M. Holthaus and S. Stenholm, Eur. Phys. J. B **20**, 451 (2001).
[24] L. Morales-Molina and S. Flach, New J. Phys. **10**, 013008 (2008).
[25] X. Luo, Q. Xie, and B. Wu, Phys. Rev. A **77**, 053601 (2008).
[26] Q. Xie and W. Hai, Phys. Rev. A **80**, 053603 (2009).

[27] L. J. Bernstein, Physica D **68**, 174 (1993).
[28] K. Sakmann, A. I. Streltsov, O. E. Alon, and L. S. Cederbaum, Phys. Rev. Lett. **103**, 220601 (2009).
[29] L. Khaykovich *et al.*, Science **296**, 1290 (2002).
[30] L. Morales-Molina, S. Flach, and J. B. Gong, Europhys. Lett. **83**, 40005 (2008).
[31] P. Hänggi and F. Marchesoni, Rev. Mod. Phys. **81**, 387 (2009).
[32] P. Hänggi and R. Bartussek, in *Nonlinear Physics of Complex Systems—Current Status and Future Trends*, edited by J. Parisi, S. C. Müller, and W. Zimmermann (Springer, Berlin, 1996), Lecture Notes in Physics No. 476.
[33] S. Folling *et al.*, Nature **448**, 1029 (2007).
[34] K. W. Madison, M. C. Fischer, R. B. Diener, Q. Niu, and M. G. Raizen, Phys. Rev. Lett. **81**, 5093 (1998).
[35] N. K. Efremidis, Phys. Rev. A **79**, 063831 (2009).
[36] M. Centurion, M. A. Porter, P. G. Kevrekidis, and D. Psaltis, Phys. Rev. Lett. **97**, 033903 (2006).
[37] A. C. Scott, P. S. Lomdahl, and J. C. Eilbeck, Chem. Phys. Lett. **113**, 29 (1985).
[38] J. C. Eilbeck, P. S. Lomdahl, and A. C. Scott, Phys. Rev. B **30**, 4703 (1984).
[39] M. Jona-Lasinio *et al.*, Laser Phys. Lett. **1**, 147 (2004).